Carola Esposito Corcione*, Francesca Gervaso, Francesca Scalera, Francesco Montagna, Tommaso Maiullaro, Alessandro Sannino and Alfonso Maffezzoli

3D printing of hydroxyapatite polymer-based composites for bone tissue engineering

DOI 10.1515/polyeng-2016-0194 Received June 7, 2016; accepted November 23, 2016; previously published online January 18, 2017

Abstract: Skeletal defects reconstruction, using custom-made substitutes, represents a valid solution to replacing lost and damaged anatomical bone structures, renew their original function, and at the same time, restore the original aesthetic aspect. Rapid prototyping (RP) techniques allow the construction of complex physical models based on 3D clinical images. However, RP machines usually work with synthetic polymers; therefore, producing custom-made scaffolds using a biocompatible material directly by RP is an exciting challenge. The aim of the present work is to investigate the potentiality of 3D printing as a manufacturing method to produce an osteogenic hydroxyapatite-polylactic acid bone graft substitute.

Keywords: biomaterials; 3D printing; hydroxyapatite; PLA.

1 Introduction

Rapid prototyping (RP) techniques have been introduced within the tissue engineering field as an alternative to conventional scaffold fabrication methods to build customized scaffolds with a highly regular and interconnected porosity and a reproducible morphology [1, 2]. These techniques allow the building of customized substitutes starting from images obtained from the patient's medical scans directly in one step, without using additional molds [3–13].

Nowadays, numerous RP techniques have been reported about the fabrication of bioresorbable scaffolds. Three-dimensional printing (3DP) heads the group with the most publications relative to new methods of scaffold

fabrication using poly(lactic acid) (PLA) and poly(lactic-co-glycolic acid) [14–16]. Among all 3DP techniques, our group focused its attention on fused deposition modeling (FDM), because it does not require the use of any solvent and offers great simplicity and flexibility in material handling and processing. Moreover, the use of FDM also reduces material residence time in the heating step and allows continuous production. Zein et al. [17] used this method to produce biodegradable poly(ϵ -caprolactone) scaffolds exhibiting various honeycomb geometries with finely tuned pore and channel dimensions of 250–700 µm.

PLA is the most extensively used biodegradable polymer for the fabrication of medical implant devices and especially tissue-engineered scaffolds. PLA is biocompatible, biodegradable, and U.S. Food and Drug Administration-approved for clinical trials. However, the cell response evaluated by in vitro cell culture models was reported to be poor on neat PLA surfaces [18]. Most cells do not attach and do not grow as vigorously as they do on surfaces containing bioactive ceramics, such as hydroxyapatite (HA) and tricalciumphosphate [19-23]. These ceramics mimic the natural apatite composition of bones and teeth. In addition, the surfaces of these ceramics are highly reactive and favor protein attachment, which also improves their bioactivity. Although bioactive ceramics alone are widely used as bone substitute materials, their clinical applications have been limited by their brittleness, even more in a porous structure for load-bearing applications [24-26].

Thus, for these uses, a composite combining the biodegradable polymers and bioactive ceramics represents a challenging strategy [27, 28]. To obtain a high-quality composite for FDM use, filaments require a high stiffness and a low melting viscosity and, consequently, good powder dispersion. The requirement for such a combination of properties makes the development of a working filament an essential task, particularly for systems loaded with ceramic powder, in which an increase of the composite viscosity should influence the homogeneity of the powder dispersion. For these reasons, additives such as surfactants and plasticizers are usually needed to obtain an acceptable composite material formulation.

Russias et al. [29], in their study, realized by robotic-assisted deposition a composite scaffold made of PLA and

^{*}Corresponding author: Carola Esposito Corcione, Dipartimento di Ingegneria dell'Innovazione, Università del Salento, via per Monteroni 73100 Lecce, Italy, e-mail: carola.corcione@unisalento.it Francesca Gervaso, Francesca Scalera, Francesco Montagna, Tommaso Maiullaro, Alessandro Sannino and Alfonso Maffezzoli: Dipartimento di Ingegneria dell'Innovazione, Università del Salento, via per Monteroni 73100 Lecce, Italy

polycaprolactone with an HA content of up to 70 wt%, with well controlled architecture and porosity. However, the composite inks were prepared by using a toxic solvent, i.e. dichloromethane.

What we want to propose in the present study is a novel method to prepare PLA-HA composite for 3D printing, specifically FDM, without using any solvent. We prepared PLA-HA pellets through premixing of HA powder with PLA pellets using a Rotomoulding machine. The pellets were processed in an extrusor in filament form that could be used for FDM.

The feasibility of using the composite PLA-HA obtained in this study with FDM technique was finally verified by fabricating a real model of a maxillary sinus reconstructed from images taken through cone-beam computer tomography.

2 Materials and methods

2.1 Experiment

A commercial HA powder (Plasma Biotal PB260R, North Derbyshire, UK) was selected as ceramic filler for the PLA

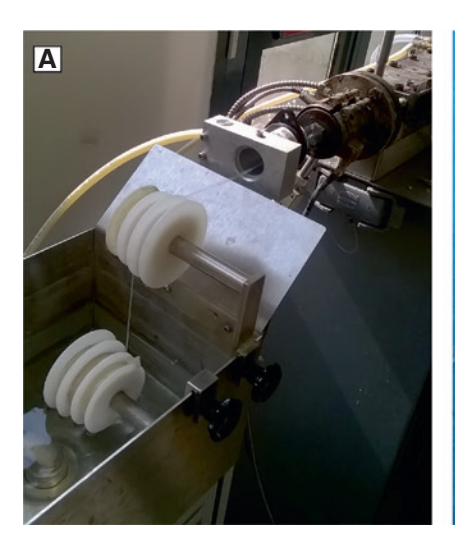
matrix. The phase composition and the particle size distribution of HA powder was evaluated by X-ray diffraction and reported elsewhere [30, 31].

PLA feedstock material was purchased from 3D Nielsen (Helsingør, Denmark) and used as the model polymer incipient. It is based on Ingeo 4043D (Natureworks LLC, Blair, Nebraska, USA) polylactide resin. The filament for the 3D printing process was obtained by melt extrusion. To obtain a homogeneous dispersion of HA in the filament, PLA pellets were coated with ceramic powder using a Rotomoulding machine (ROTOMOULD ALPHA, Salentec, Lecce, Italy). This laboratory equipment is usually used for rotational molding of prototypes and preseries products. In this case, PLA and HA were inserted in the mold and rotated for a defined time, at a specific temperature, close to PLA melting temperature $(T_m = 145^{\circ}\text{C})$. Different process conditions were tested to optimize the mixing. The optimal parameters, i.e. temperature, time, and rotation rate, are listed in Table 1 for each mixing step. After Rotomoulding treatment, PLA was homogeneously coated by an HA layer.

A filament suitable for 3D printing was obtained by melt extrusion with a twin screw extruder (Haake reomix 600/610, Rezzato (BS), Italy) (Figure 1A and B).

Table 1: Optimal Rotomould parameters to obtain a homogeneous HA coating on PLA pellets.

	Temperature (°C)	Time (min)	Rpm first direction (rpm)	Rpm second direction (rpm)
First step	170	30	40	60
Second step	180	10	40	60
Third step	Air cooling cycle	15	40	60



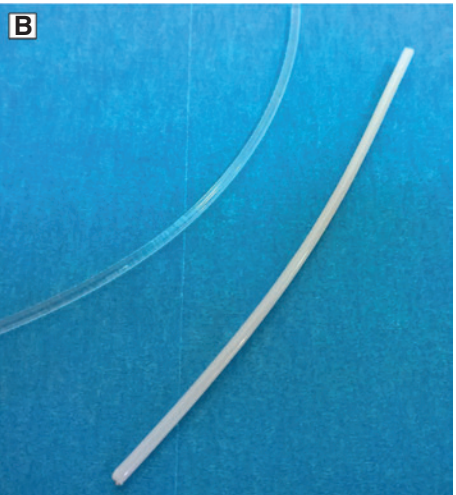


Figure 1: (A) Picture of PLA and PLA/HA composite extrusion process. (B) Picture of PLA and PLA/HA (white) filament.

Table 2: Process parameters for the realization of the PLA and PLA/

PLA	PLA/HA
60	30
185	220
200	210
180	190
180	170
	60 185 200 180

To obtain a filament with a diameter of 1.75 mm, two different temperature profiles and screw speeds were used, changing them for pure PLA and PLA/HA composite. Immediately at the exit from the circular die (3 mm in diameter), the material was water-cooled and coiled on a spool. Process parameters are summarized in Table 2. Simple bar-shaped samples (4 mm in height, 12 mm in width, 85 mm in length) were realized by using a 3DPRN LAB 3D (TIPS, Castiglione M.R. (TE), Italy) (Figure 2A and B). All samples were built according to the parameters reported in Table 3.

To verify the suitability of the materials and the additive manufacturing technique for producing bone scaffolds of complex shape, a maxillary sinus was also fabricated by 3D printer. Human clinical images, acquired by 3D cone-beam computer tomography, were converted in a 3D CAD representation of a bone defect, i.e. a maxillar sinus, as an example of custom-made bone substitute. Finally, the 3D printing parameters, i.e. nozzle size and layer height were set equal to 0.2 mm and 0.1 mm, respectively, to obtain a porous structure.

2.2 Characterization

The composite morphology was characterized by SEM micrographs (Zeiss evo 40, Oberkochen, Germany) equipped with energy-dispersive X-ray (EDX) spectroscopy

Table 3: Building parameters of 3DPRN LAB 3D (TIPS).

Nozzle size (mm)	0.4
Layer height (mm)	0.2
Perimeters	3
Top/bottom layers	3
Infill (%)	100
Nozzle speed (mm/s)	50
Nozzle temperature (°C)	200

system (Bruker XFlash detector 5010, Billerica, MA, USA) allowing the evaluation of HA distribution and dispersion on fracture surfaces.

Thermogravimetric analysis was performed on the extruded composite filament to evaluate the HA content. The analysis was also repeated on the pure PLA filament as a reference. A TGA/DSC1 Star and System, Mettler Toledo, Zürich, Switzerland, was used in the range 20°C-800°C at a heating rate of 10°C/min.

The three-point bending tests were conducted with a Lloyd (Lloyd LR5K, Fareham, UK) universal testing machine on five bar-shaped samples for each material, i.e. pure PLA and PLA/HA. The applied velocity of the bending load was 1.7 mm/min. Flexural modulus and strength were calculated from the experimental data according to the formula reported in the ASTM D790 standard.

The 3D-printed maxillary sinus was then measured with a digital caliper to assess the real dimensions of the object and compare them to the fabrication dimension imposed on the FDM machine. Finally, SEM images of the printed sinus were acquired to verify the pore size and the porosity interconnection.

3 Results and discussion

The cross-section of PLA/HA composites was first observed by SEM and then analyzed by EDX mapping,



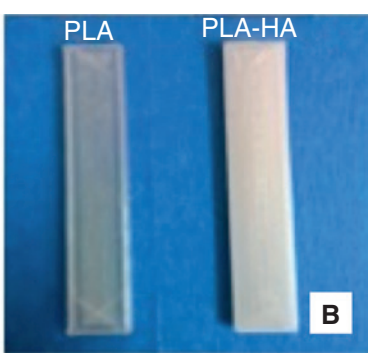


Figure 2: (A) 3DPRN LAB 3D during the layer by layer deposition and (B) PLA (left) and PLA-HA (right) bars realized.

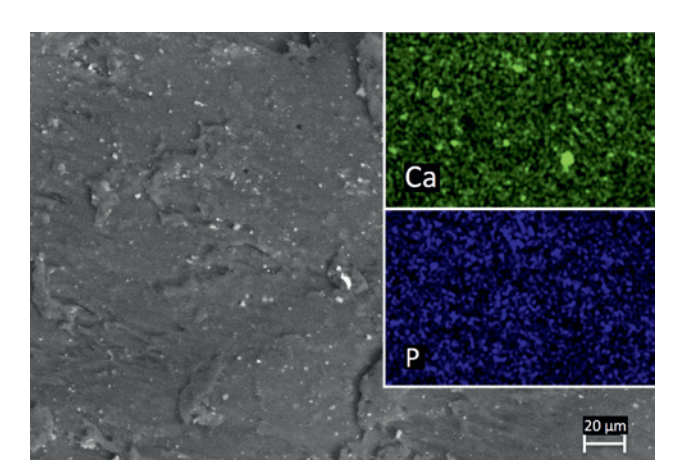


Figure 3: SEM images of PLA/HA composite with elemental mapping (top view).

and the obtained images are reported in Figure 3. It can be noticed that the procedure used to prepare PLA/HA composites led to a good dispersion of HA particles within the polymeric matrix. The EDX mapping showed a high Ca

and P content, demonstrating a homogeneous presence for HA particles.

A comparison between the TGA curves obtained for the neat PLA and PLA/HA composite filaments is reported in Figure 4. The results evidenced a solid residue of HA for the composite 3D printing filament of 3.8% wt., whereas the neat PLA filament showed a residue of 0.39% wt. Consequently, it is possible to assume that a HA content of about 3.4% is present in the composite 3D-printed filament.

The Rotomoulding route for material processing allowed a good dispersion of the filler with a minimal loss of the starting percentage of inorganic component. Russias et al. [29] obtained a higher content of HA, but with a different technique that needed the use of a very toxic solvent (methylene chloride). Further experiments on this topic have already been started and are focused on increasing the HA percentage by directly mixing the powders to the polymer using an extruder.

The flexural tests performed on the neat and filled PLA flexural specimens, according to ASTM D790 standards,

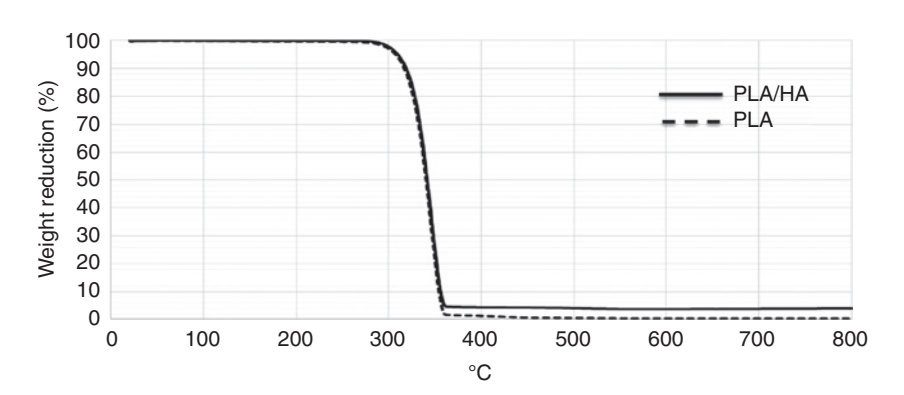


Figure 4: TGA curves of neat PLA and PLA/HA composite.

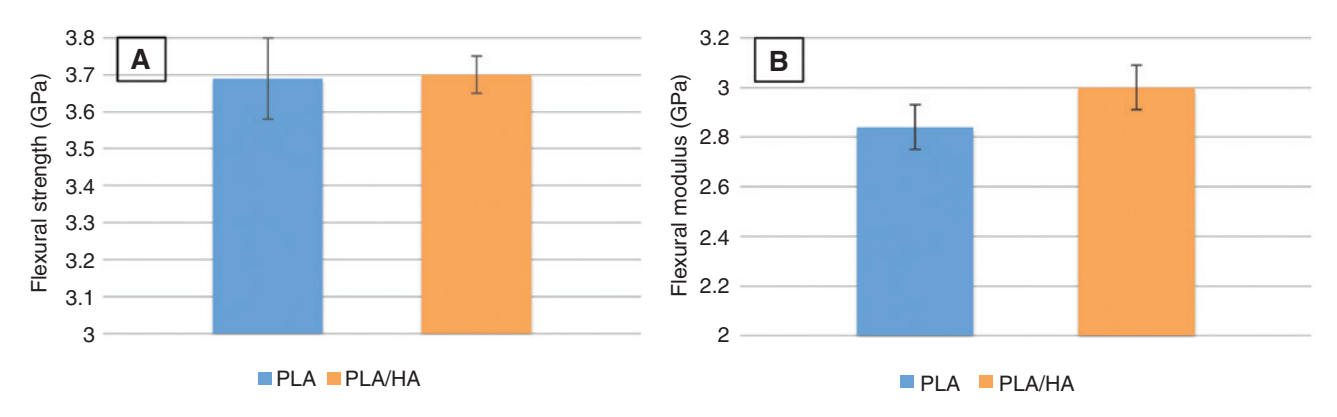


Figure 5: Flexural test results of neat and filled PLA specimens: (A) flexural strength and (B) flexural modulus.

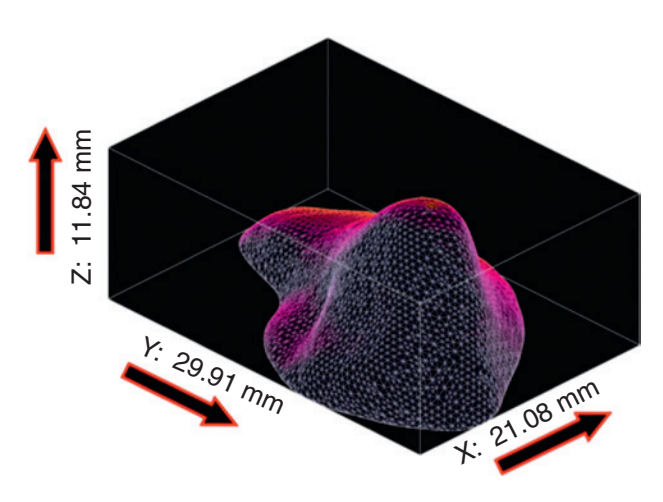


Figure 6: The *.stl model dimensions of the maxillary sinus.

show that the composite material has a slightly higher modulus than those of pure PLA, whereas the strength is about the same (Figure 5A and B).

The maxillary sinus was correctly fabricated by (i) acquiring the anatomical images using 3D cone-beam computer tomography, (ii) exporting the clinical data into a commercial software (Mimix, Materialize) for the CAD three-dimensional virtual reconstruction of the anatomy, (iii) generating a virtual file in the *.stl format suitable for 3D printing (Figure 6). In Figure 6, the *.stl virtual model sizes are reported as the maximum x-y-zdimensions.

The 3D-printed porous maxillary sinus was properly fabricated and is shown in Figure 7A. The real model was measured with a digital caliper and the measured x, y, z dimensions were slightly higher than the nominal ones (error < 1%). The resulting porosity of the sinus was interconnected and higher than 300 µm, which has been

reported [32, 33] as a good pore size dimension for bone regeneration.

This is an important result evidencing the feasibility of FDM to realize scaffolds with a complex shape without using any toxic solvent during the process. Although in other works [29], a higher percentage of HA was obtained in the scaffold; this technique, which used 3D inks, is not suitable to directly pattern complex structures with large unsupported regions such as overhanging features.

4 Conclusion

The aim of this research was to develop a solvent-free process to produce an HA polymer-based composite material suitable for 3D printing processes to realize customized scaffolds for tissue engineering. The homogenous PLA/HA starting composite material was first prepared, not as usual by mixing them with a solvent, but through a Rotomoulding machine, which allowed the production of a composite in the form of pellets, and processed to obtain a wire suitable to feed a FDM machine. In the composite PLA/HA filament, the HA content was homogeneously distributed within the PLA matrix as confirmed by SEM and EDX analyses. Although a relatively small content of HA was added, the flexural modulus already showed a slight increase if compared with the pure PLA. The HA content surely has to be increased and further studies are already on-going in this direction. However, the 5% HA content used in this study is, in our opinion, a sufficient amount to assess the feasibility of the method. Finally, clinical images of a maxillary sinus obtained by conebeam computer tomography were properly converted in the suitable format and successfully used to fabricate a



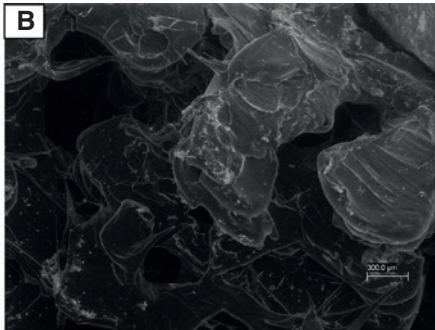


Figure 7: Picture (A) and SEM image (B) of the porous three-dimensional maxillary sinus fabricated by 3D printing starting from clinical images acquired by 3D cone-beam computed tomography.

real three-dimensional maxillary sinus model using the developed composite material by 3D printing.

References

- [1] Widmer MS, Mikos AG. In Frontiers in Tissue Engineering, Patrick Ir CW, Mikos AG, McIntire LV, Eds., Elsevier, New York, 1998.
- [2] Hutmacher DW. Biomaterials 2000, 21, 2529-2543.
- [3] Esposito Corcione C, Greco A, Maffezzoli A. J. Therm. Anal. Calorim. 2003, 72, 687-693.
- [4] Esposito Corcione C, Greco A, Maffezzoli A. J. Appl. Polym. Sci. 2004, 92, 3484-3491.
- [5] Licciulli A. Esposito Corcione C. Greco A. Amicarelli V. Maffezzoli A. J. Eur. Ceramic Soc. 2004, 24, 3769-3777.
- [6] Licciulli A, Esposito Corcione C, Greco A, Amicarelli V, Maffezzoli A. J. Eur. Ceramic Soc. 2005, 25, 1581-1589.
- [7] Esposito Corcione C, Greco A, Licciulli A, Maffezzoli A. J. Mater. Sci. 2005, 40, 1-6.
- [8] Esposito Corcione C, Montagna F, Greco A, Licciulli A, Maffezzoli A. Rapid Prototyp. J. 2006, 12, 184-188.
- [9] Esposito Corcione C, Greco A, Maffezzoli A. Polym. Eng. Sci. 2006, 46, 493-502.
- [10] Scalera F, Esposito Corcione C, Montagna F, Sannino A, Maffezzoli A. Ceram. Int. 2014, 40, 15455-15462.
- [11] Esposito Corcione C. J. Polym. Eng. 2014, 34, 85-93.
- [12] Esposito Corcione C, Striani R, Montagna F, Cannoletta D. Polym. Advan. Technol. 2015, 26, 92-98.
- [13] Birtchnell T, Urry J. Futures 2013, 50, 25-34.
- [14] Rezwan K, Chen QZ, Blaker JJ, Boccaccini AR. Biomaterials 2006, 27, 3413-3431.
- [15] Navarro M, Aparicio C, Charles-Harris M, Ginebra MP, Engel E, Planell JA. Adv. Polym. Sci. 2006, 200, 209-231.
- [16] Taboas JM, Maddox RD, Krebsbach PH, Hollister SJ. Biomaterials 2003, 24, 181-194.

- [17] Zein I, Hutmacher DW, Tan KC, Teoh SH. Biomaterials 2002, 23, 1169-1185.
- [18] Persson M, Lorite GS, Kokkonen HE, Cho SW, Lehenkari PP, Skrifvars M, Tuukkanen. J Colloids Surf. B 2014, 121, 409-416.
- [19] Sui G, Yang X, Mei F, Hu X, Chen G, Deng X, Ryu S. J. Biomed. Mater. Res. Part A 2007, 82A, 445-454.
- [20] Cui Y, Liu Y, Cui Y, Jing X, Zhang P, Chen X. Acta Biomater. 2009, 5. 2680.
- [21] Aydin E, Planell JA, Hasirci V. J. Mater. Sci. Mater. Med. 2011, 22, 2413.
- [22] Hong Z, Zhang P, He C, Qiu X, Liu A, Chen L, Chen X, Jing X. Biomaterials 2005, 26, 6296.
- [23] Kikuchi M, Koyama Y, Takakuda K, Miyairi H, Shirahama N, Tanaka J. J. Biomed. Mater. Res. 2002, 62, 265.
- [24] Rizzi SC, Heath D, Coombes A, Bock N, Textor M, Downes S. J. Biomed. Mater. Res. 2001, 55, 475.
- [25] Kim S, Sun Park M, Jeon O, Yong Choi C, Kim B. Biomaterials 2006, 27, 1399.
- [26] Wang H, Li Y, Zuo Y, Li J, Ma S, Cheng L. Biomaterials 2007, 28, 3338-3348.
- [27] Hutmacher DW, Schantz T, Zein L, Ng KW, Teoh SH, Tan KC. J. Biomed. Mater. Res. 2001, 55, 203-216.
- [28] Landers R, Muhlhaupt R. Macromol. Mater. Eng. 2000, 282, 203-216.
- [29] Russias J, Saiz E, Deville S, Gryn K, Liu G, Nalla RK, Tomsia AP. J. Biomed. Mater. Res. A 2007, 83, 434-445.
- [30] Trantolo DJ, Lewandrowski KU, Gresser JD, Wise DL. Biomater. Eng. Dev. 2000, 2, 291-308.
- [31] Scalera F, Gervaso F, Sanosh KP, Sannino A, Licciulli A. Ceram. Int. 2013, 39, 4839-4846.
- [32] Kuboki Y, Jin Q, Takita H. J. Bone Joint Surg. Am. 2001, 83A,
- [33] Tsuruga E, Takita K, Itoh H, Wakisaka Y, Kuboki Y. J. Biochem. 1997, 121, 317-324.